Dimensional analysis parameters of turbulence in the wake of a square cylinder

Cite as: AIP Conference Proceedings **2323**, 030003 (2021); https://doi.org/10.1063/5.0041434
Published Online: 08 March 2021

Vitalii Yanovych, Daniel Duda, and Václav Uruba

Dimensional Analysis Parameters of Turbulence in the Wake of a Square Cylinder

Vitalii Yanovych[1, a)], Daniel Duda[1, b)] and Václav Uruba[1, 2, c)]

[1]*University of West Bohemia in Pilsen, Univerzitní 22, Pilsen, Czech Republic*
[2]*Institute of Thermomechanics, Czech Academy of Sciences, Dolejškova 5, Prague, Czech Republic*

[a)]Corresponding author: yanovych@kke.zcu.cz
[b)]dudad@kke.zcu.cz
[c)]uruba@kke.zcu.cz

Abstract. In this article, we show the results of a study of the structure of a turbulent flow behind a square cylinder. Namely, for the series of points that have the highest standard deviation value. During the experiment, we were changing the position of the square cylinder relative to the total flow. Experimental data were obtained using Constant Temperature Anemometry. As a result of the analysis, we obtained graphical distributions of the main parameters of the turbulent flow. They revealed that the maximum value of the Reynolds number based on the Taylor micro-scale is observed exactly at the cylinder angle of 30° and 45°. It was also found that the distribution of the energy dissipation rate, depending on the angle of rotation of the cylinder, has a certain sinusoidal character with local peak values. The results of the analysis also showed that the distribution of values of dissipation scale and dissipation time at some distance from the cylinder has the largest range of their values.

INTRODUCTION

The study of the transverse flow of a viscous fluid over a cylinder is one of the classical problems of mechanics. It is known that in the range of the Reynolds number $Re_d \approx 60 - 5 \cdot 10^5$, calculated from the cylinder diameter d and the incident flow velocity U, behind the cylinder occurs periodic formation of regular vortices - Karman´s vortex trail. Starting from $Re_d \approx 10^3$ the frequency of vortex disruptions is describing by Strouhal number St. This value remains almost unchanged and for unlimited external flow is $St \approx 0.21$.

The study of vortex structures resulting from the flow of a square cylinder is of great importance in various engineering fields. In practice, this is due to the design of structures for various industries. In particular, the use of aluminum structures in various scientific experiments has become widespread. These structures are generally exposed to a variety of fluid or air flows.

Therefore, predicting the characteristics of a flow passing a square cylinder is an urgent task. In addition, this phenomenon is complex. Because it involves the separation and reconnection of vortices, the unstable vortex outflow and its bimodal behavior, high turbulence, and large-scale turbulent structures. One of the main small-scale characteristics of turbulence is the rate of energy dissipation. Which determines kinetic energy transport among many large-scale turbulent structures.

Traditionally, the Constant Temperature Anemometry (CTA) method has been used to analyze the structure of turbulent flow with reference to the Taylor hypothesis [1]. The Particle Image Imaging (PIV) is also widely used to analyze and visualize the various structures of turbulent flows [2, 3]. In particular, in the works of Saarenrinne and Piirto, Sheng and others. [4] and Jong et al. [5] used the method (PIV) to determine the rate of dissipation.

It is worth noting that many researchers have devoted their attention to the study of flow through a square cylinder. In particular, the velocity of energy dissipation by a cylinder was investigated in articles [6-8]. Whereas, for example, Mi and Anthony [9] concentrated their studies on the measuring mean velocity of turbulent dissipation at $Re = 3000$.

19th Conference on Power System Engineering
AIP Conf. Proc. 2323, 030003-1–030003-7; https://doi.org/10.1063/5.0041434
Published by AIP Publishing. 978-0-7354-4067-8/$30.00

Experimental Details

Experimental studies were conducted in an open wind tunnel. Which was developed at the University of West Bohemia (Figure 1(a)) [10, 11]. The scheme of the experimental study is shown in Figure 1(b). The test section had dimensions of 305 mm (width) × 204 mm (height) × 750 mm (length), respectively. For the experimental study, the aluminum profile of the company ALUTEK KK was selected. This profile has the shape of a square cylinder whose height is h = 200 mm, the size of the side of the cylinder d = 45 mm. Thus the ratio of the sides of the cylinder is 4.4 and an area blockage of about 15%. The center of the square cylinder is located at a distance of 3.3 d and 5.3 d, respectively, from the wall and the inlet of the test section, as shown in Figure 1(b). Lower part of the cylinder was at a distance $l/d \approx 0.11$ from the bottom of the test section. When conducting experimental studies, change the angle of attack of the cylinder α to a total flow of 0° to 45° with steps 15°. The mean flow velocity was U = 5 m·s^{-1}, which corresponds to a Reynolds number based on the dimensions of cylinder $Re_d \approx 1.5 \cdot 10^5$.

The measuring plane was located at the rear of the cylinder at a distance of 100 mm. This distance was chosen to avoid areas of space containing backflows. The distance between the measuring points was 10 mm. Constant Temperature Anemometry (CTA) with a speed sensor of type 55P15 (for measuring stream-wise component of the flow) was used to study the structure of the turbulent flow behind the cylinder. Sample Rate to measure was 60 kHz and a single measurement time was 10 s. Filtration of the obtained data was carried out with the parameters: for High-pass filter - 10 Hz and for Low-pass filter it was 30 kHz.

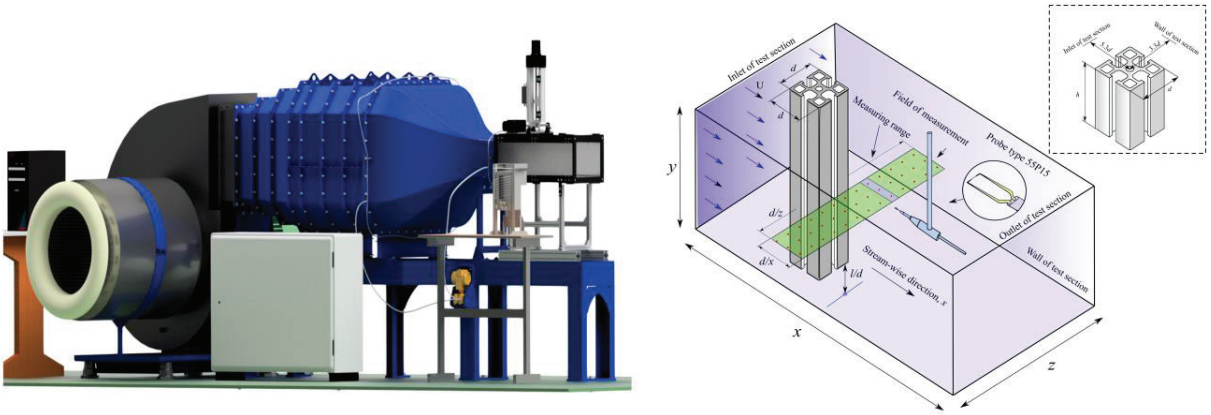

FIGURE 1. (a) The experimental model of the developed aerodynamic tunnel. (b) Scheme of experimental study. Where d is the size of the side of a square cylinder. d/z and d/x is measurement point coordinates with respect to the x and z axes.

DIMENSIONAL ANALYSIS

First, we investigated the distribution of the flow velocity u and the standard deviation σ_u behind the cylinder at a distance x/d = 2.2, changing the angle α (Figure 2). Measurements were made for the entire measuring area which is shown in Figure 1 (b).

It is obvious that immediately behind the cylinder in the range from z/d = 2.6 to z/d = 4.3 there is a sharp decrease in the flow velocity. In this range, the minimum value of u is u = 3.2 - 3.7 m·s^{-1}. While outside this range, the value of u increases by 35% of the set speed U and ranges from 6.1 m·s^{-1} to 7 m·s^{-1}. This feature is caused by a sharp change in the static and dynamic flow pressure in the section between the cylinder and the walls of the test section.

The obtained graphical distribution of σ_u depending on the angle α showed that behind the cylinder there is some local region of minimum values at z/d = 3.5 - σ_u = 1.2-1.4. Whereas at z/d = 2.6 and z/d = 4.3 coordinates maximum values of σ_u from 1.6 to 1.9 are observed. Outside this range, there is a significant decrease in σ_u to 0.3. This pattern is logical. Because maximum values of σ_u are some indication of the most active sections of the flow behind the cylinder.

Therefore, it is of considerable interest to further study the structure of the turbulent flow of a series of points along the straight line at z/d = 2.6 (in stream-wise direction) from x/d = 2.2 to x/d = 3.3. For example, the algorithm for calculating turbulent flow parameters at one of the measuring points is given below. We chose the first measuring point with the coordinates x/d = 2.2 to z/d = 2.6.

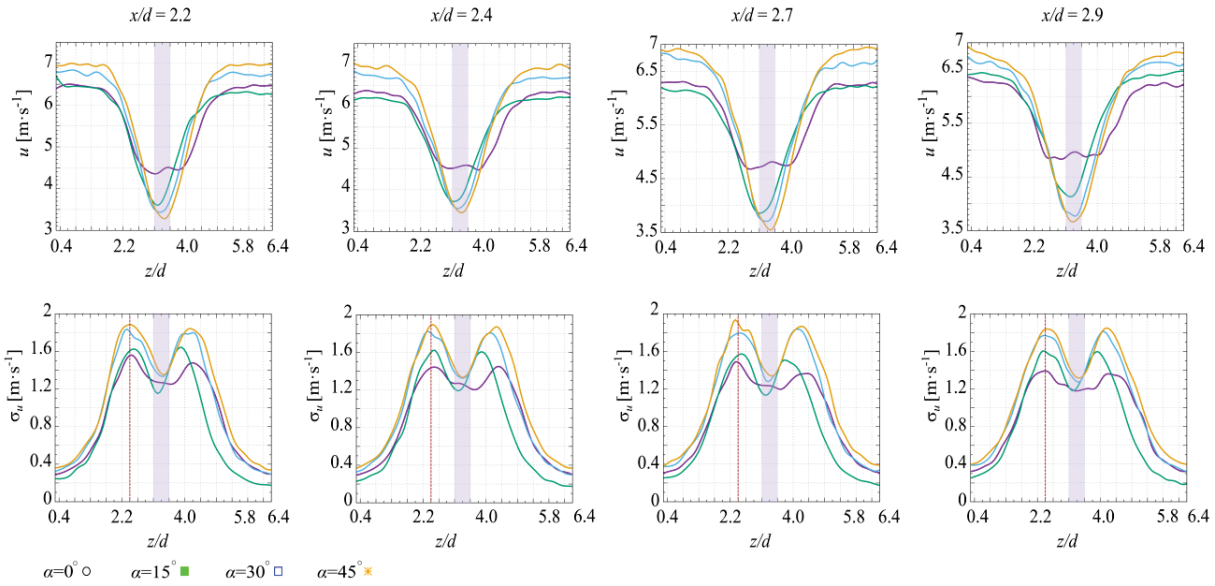

FIGURE 2. Flow velocity u and standard deviation distribution σ_u depending on angle α and distance from cylinder. Blue color shows the conditional placement of the cylinder. The red dashed line shows the range of the largest values of the standard deviation (these points were used for further analysis).

The structure of turbulent flow has a wide range of vortex structures. Therefore, the Fourier spectral analysis (PSD) was used to estimate the turbulent flow energy, characterizing the change in the power spectral density in the inertial interval (Figure 3 (a)). The inertial interval is limited by the low and high frequencies. Low frequencies are associated with large-scale eddy structures. Whereas, high frequencies are associated with small-scale vortices and characterize the dissipation of kinetic energy in a turbulent flow.

The probability distribution of the amplitudes of fluctuations is subject to Gaussian law. From the behavior of the probability density function (PDF), you can determine the characteristic spatial or temporal scale. This is determined by the step at which the PDF of the signal loses the Gaussian distribution form. In the presence of heterogeneity of turbulent processes, we observe significant distortion of the PDF.

Kolmogorov's theory considers structural functions (moments) of order q for the difference of velocities on a spatial scale [12]:

$$\delta_l u = u(x+l) - u(x), S_q(l) \equiv \left\langle \left| \delta_l u \right|^q \right\rangle, \tag{1}$$

or for time scale τ:

$$\delta_\tau u = u(t+\tau) - u(t), S_q(\tau) \equiv \left\langle \left| \delta_\tau u \right|^q \right\rangle. \tag{2}$$

The study of structural functions is tantamount to the study of the function of the distribution of turbulent oscillations. From a practical point of view, it is easier to study structural functions. Because they can be built on based experimental data. The method of structural functions allows to describe in detail the heterogeneity of the distribution at different scales of the process. According to Kolmogorov K41 theory, there is a certain statistical quasi-equilibrium fluctuation for isotropic developed turbulence and Gaussian distribution of instantaneous fluctuations in flow velocity.

In the inertial interval of the turbulent cascade $\eta << l << L$ at large Reynolds numbers all statistically averaged moments $S_q(l)$ velocity fields u at scale l depend only on the average dissipation rate ϵ and this scale l. In turn, the magnitude characterizes the dissipative scale and the global scale of the vortex structures. The dynamics of the inertial range does not depend on the method of generating turbulence and is determined by the invariance of the energy flow through this interval. That is, in fact, the average energy flow remains constant. The laws of scale invariance (scaling) for $S_q(l)$ and for dissipation energy ϵ are widely used in practice:

$$S_q(l) \propto \left(\delta_l u\right)^q \propto l^{(q/3+\tau(q/3))}, \varepsilon_l^q \propto l^{\tau(q)} \tag{3}$$

In the K41 model, the fact of homogeneity of turbulent processes is reflected by the function *q/3*. Also, the function of *q/3* indicates an irregular redistribution of energy in turbulent cascades and a violation of the local homogeneity of flow turbulence. The so-called alternation of vortices with quasi-laminar flows. This non-linearity also indicates a deviation of the PDF from Gaussian law. In the Kolmogorov K41 model, the assumption of the local nature of turbulence is fundamental. This means that in the inertial interval, the change in energy at this scale is determined by the interaction of the vortices alone. Which have close values of wavenumbers and interact for a long time. The interaction of vortices with different sizes is small. In the K41, turbulent vortices of each scale uniformly fill the entire space. According to Kolmogorov's studies, with developed isotropic turbulence in the inertial range, the energy flow spectrum has a dependence $f^{5/3}$. Eulerian power spectral densities of velocity fluctuations and probability density functions of the velocity fluctuations shows on Figure 3.

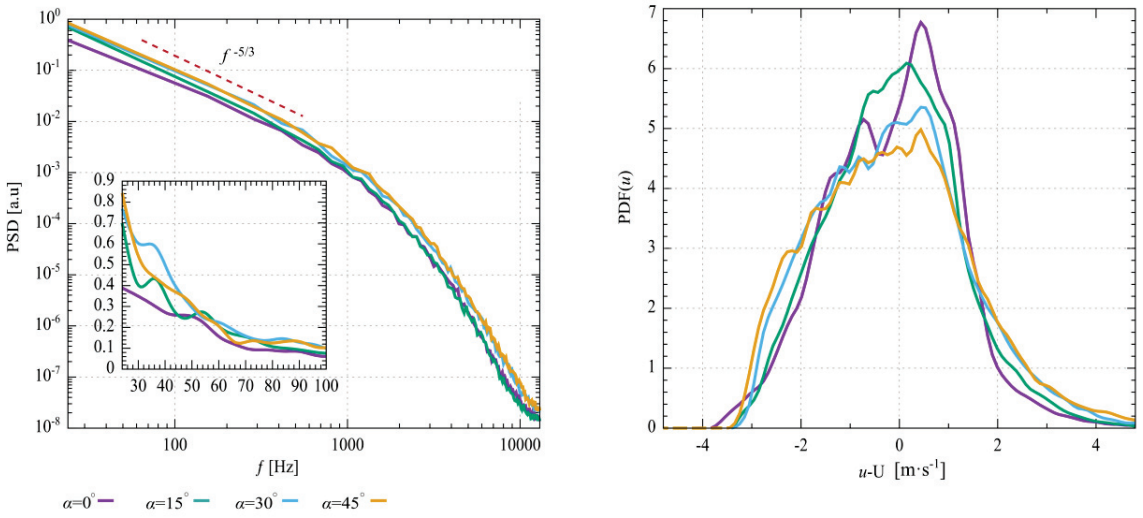

FIGURE 3. (a) Eulerian power spectral densities of velocity fluctuations (PSFs). (b) Probability density functions of the velocity fluctuations (PDFs).

For study the structure of the turbulent flow, the Eulerian autocorrelation function R_{uu} (normalized to standard deviation) was used.

$$R_{uu}(t) = \frac{\langle u(t+\Delta t)\cdot u(t)\rangle}{\sigma_u^2} \tag{4}$$

Using the autocorrelation function, we can easily determine the lifetime of the largest vortices (Figure 4 (a)). This is the distance where the autocorrelation coefficient is equal to zero or becomes negative.

Mean vortex lifetime or Eulerian time scale T_E was found using the cumulative integral of the autocorrelation function.

$$T_E = \int_0^\infty R_{uu}(t)dt \tag{5}$$

Then the Eulerian length scale was found from dependency $L=T_E/\sigma_u$.

The analysis figure 4 (b) showed that, depending on the angle α, the T_E value varies: for α = 0° - $T_E \approx$ 6.6 ms; for α = 15° - $T_E \approx$ 6.9 ms; for α = 30° - $T_E \approx$ 7.3 ms and for α = 45° - $T_E \approx$ 6.9 ms. But, the dynamics of change for the Eulerian length scale L are somewhat different, in particular: for α = 0 - $L \approx$ 10 mm; for α = 15° - $L \approx$ 11 mm; for α = 30° - $L \approx$ 12 mm and for α = 45° - $L \approx$ 13 mm.

To determine the energy characteristics of the turbulent processes observed in the experiment, an analysis of the features of structural functions were performed. High-order structural functions allow us to characterize the properties of flow heterogeneity on a small scale. The second-order Eulerian longitudinal structure function S_{uu}^2 allows determining the dissipation rate ϵ of turbulent flow. In our case, the second-order structural function was determined by the relation $S_{uu}^2(t) = C(\varepsilon t)^{2/3}$ where C =2.1 [12].

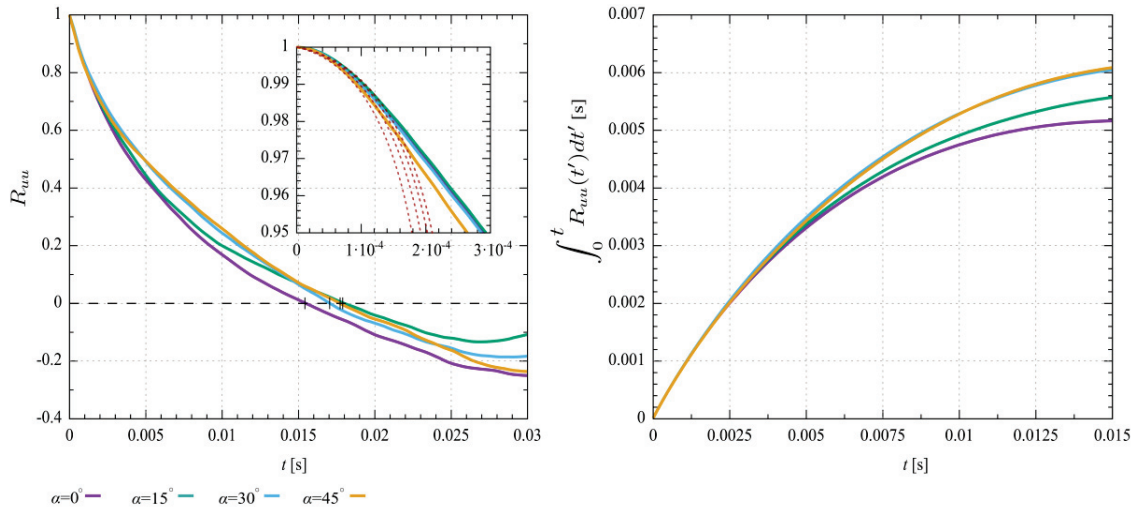

FIGURE 4. (a) Autocorrelation function Eulerian R_{uu} of the streamwise velocity. (b) Cumulative integral of R_{uu}, whose asymptotic value gives the estimation of the integral scale L of the turbulence.

Based on the values found ϵ we can easily find the values the dissipation scale η and the dissipation time τ_η and Reynolds number R_λ based on the Taylor micro-scale:

$$\eta = \left(\nu^3 / \check{n}\right)^{1/4}, \tag{6}$$

$$\tau_\eta = \left(\nu / \check{n}\right)^{1/2}, \tag{7}$$

$$R_\lambda = \left(\sigma_u \lambda\right) / \nu, \tag{8}$$

were $\lambda = \sigma_u \sqrt{15\nu / \check{n}}$ the Taylor micro-scale of the flow.

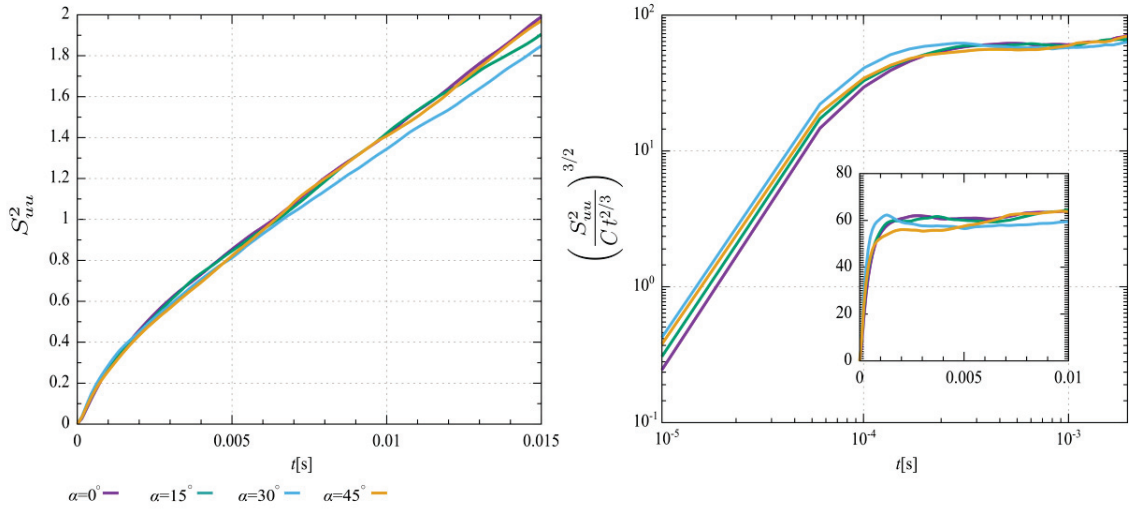

FIGURE 5. (a) Second order structure function. (b) Estimate of turbulent kinetic energy dissipation rate ϵ based on the estimated structure function dependence on time-difference t, minor panel shows the same data in linear plot.

Figure 5 was used to determine the value dissipation rate ϵ at the point with coordinates x/d=2.2 i z/d=2.6: for α = 0° - $\epsilon \approx 66.4$ m^2·s^{-3}; for α = 15° - $\epsilon \approx 63.3$ m^2·s^{-3}; for α = 30° - $\epsilon \approx 60.7$ m^2·s^{-3} and for α = 45° - $\epsilon \approx 65.6$ m^2·s^{-3}.

The obtained experimental data allowed us to establish that the change in angle α has no significant effect on the value dissipation scale η. Because in the range changes from $\alpha = 0°$ to $\alpha = 45°$ - dissipation scale is approximately same $\eta \approx 85$ μm. It will then be logical that the angle α also has no significant effect on the magnitude dissipation time τ_η. At different values of the angle α dissipation time has a values in the interval 0.45-0.48 ms.

However, an analysis of the Reynolds number based on Taylor micro-scale showed that at an angle $\alpha = 45°$ the observed maximum value $R_\lambda \approx 431$. And for other values of the angle α Reynolds number is lower: for $\alpha = 0°$ - $R_\lambda \approx 294$; for $\alpha = 15°$ - $R_\lambda \approx 331$ and for $\alpha = 30°$ - $R_\lambda \approx 392$.

General characteristics of the parameters of the turbulent flow at a point with coordinates $x/d = 2.2$ to $z/d = 2.6$ depending on the angle α are shown in table 1.

TABLE 1. The parameters of the turbulent flow at the measuring point of the point at $x/d = 2.2$ and $z/d = 2.6$ at the $U = 5$ m·s^{-1}

α[°]	σ_u [m·s^{-1}]	T_E [ms]	L [mm]	ϵ [m^2·s^{-3}]	η [μm]	τ_η [ms]	λ [mm]	R_λ
0	1,5	6,6	10	66,4	85	0,47	2,8	294
15	1,6	6,8	11	63,3	85	0,48	3,1	331
30	1,7	7,3	12	60,7	86	0,49	3,4	392
45	1,8	6,9	13	65,6	85	0,48	3,5	431

We made a similar calculation for all points of the coordinate range at $z/d = 2.2$ from $z/d = 2.2$ to $x/d = 3.3$. On the basis of the analysis a series of graphs was obtained. These graphs show how the parameters of the turbulent flow change depending on the distance x/d and the angle α (Figure 6).

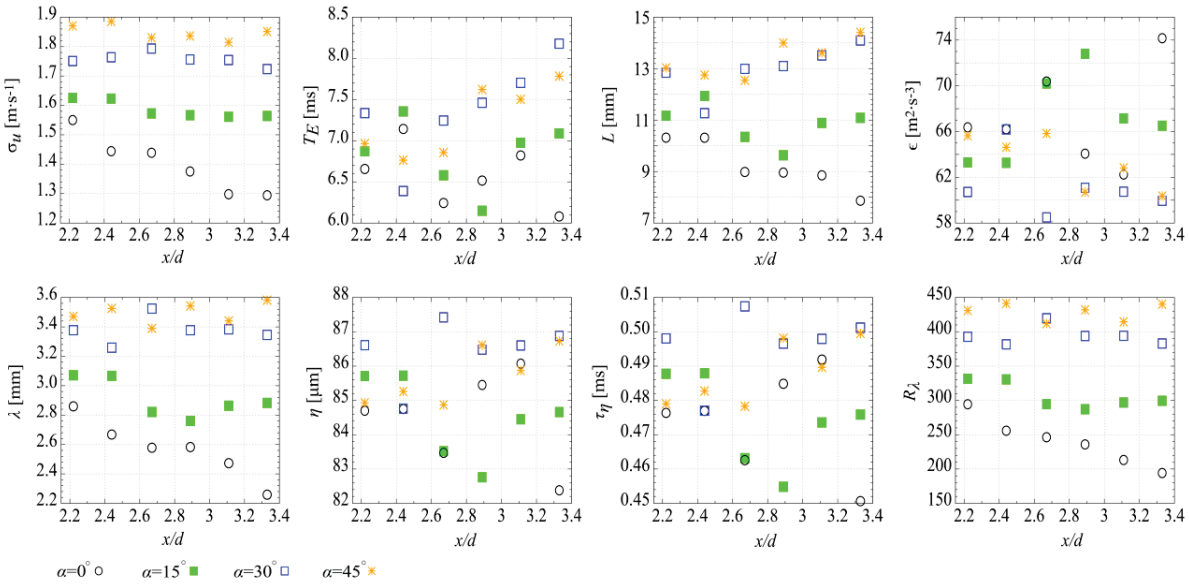

FIGURE 6. Flow characteristics in stream-wise direction. The transverse coordinate z/d is fixed to 2.2, and it is depicted in figure 2 as a vertical dashed line.

Figure 6 shows that the size of the angle α significantly influences the value standard deviation. With increasing distance from the cylinder x/d and depending on the angle α, the range of magnitudes σ_u increases. However, it is interesting that at an angle $\alpha = 30°$ and $\alpha = 45°$, the values of σ_u do not change significantly and are similar. It should be noted that a similar trend is observed for T_E, L, λ as well as for R_λ.

The maximum value of the Eulerian time scale is observed at the end of the measurement series, that is, at a maximum distance from the cylinder $T_E = 8.2$ ms at $\alpha = 30°$. A similar trend is observed for the Eulerian length scale at $x/d = 3.3$ and $\alpha = 30°$ - $L = 14$ mm.

An interesting pattern is the distribution of the energy dissipation rate. We can see, that depending on the angle α and with increasing distance from the cylinder, observe some peak values: for $\alpha = 0°$ and x/d=2.7 - $\epsilon \approx 70$ m^2·s^{-3}; for

α = 15° and x/d=2.9 - $\epsilon \approx 73$ m^2·s^{-3}; for α = 30° and x/d=2.4 - $\epsilon \approx 66$ m^2·s^{-3}; for α = 45°and x/d=2.7 - $\epsilon \approx 66$ m^2·s^{-3}. This is a natural phenomenon that shows the effect of the Karman´s vortex trail behind the cylinder.

Some interest situation for magnitudes dissipation scale and dissipation time we can observe in the measuring point with coordinates x/d=2.7 and z/d = 2.2.

At the measuring point with coordinates x/d = 2.7 and z/d = 2.2 we can observe some interesting situations regarding for magnitudes dissipation scale and dissipation time. With the given coordinates, the largest range of values of the given parameters is observed: for $\eta \approx$ 83-87 μm and for $\tau_\eta \approx$ 0.46-0.51 ms.

The experimental data obtained allowed us to establish the maximum value Reynolds number based on the Taylor micro-scale is observed at the corners α = 30° and α = 45° and is approximately equal $R_\lambda \approx 400$.

CONCLUSION

We used the Constant Temperature Anemometry method to analyze the parameters of the turbulent flow around a square cylinder. The aluminum cylinder made by ALUTEK KK was used as a square cylinder. The main focus of this article was on the study of turbulence characteristics behind the cylinder. Namely, for the range of measuring points with coordinates at z/d = 2.2 from x/d =2.2 to x/d =3.3. Because this is where the highest standard deviation is observed. Based on the experimental data we obtained, we calculated Eulerian time and length scale, dissipation rate, Taylor micro-scale, dissipation scale, dissipation time and Reynolds number based on Taylor micro-scale. It should be noted that the results of the calculations clearly shows the significant influence of the angle of rotation of the cylinder α on the values of the studied parameters.

In the future, we plan to continue the study of the structure of turbulent flows near the edges of a square cylinder at different Reynolds numbers.

ACKNOWLEDGMENTS

This work was supported by the project of Technology Agency of the Czech Republic TACR No. TH02020057 “Program Epsilon”.

REFERENCES

1. M. Bourgoin, C. Baudet, S. Kharche et al, “Investigation of the small-scale statistics of turbulence in the Modane S1MA wind tunnel”, CEAS Aeronaut J **9**, 269-281 (2018).
2. D. Duda, J. Bém, V. Yanovych, P. Pavlíček and V. Uruba, “Secondary flow of second kind in a short channel observed by PIV”, European Journal of Mechanics, B/Fluids **79**, 444-453 (2020).
3. J. Bém, D. Duda, J. Kovařík, V. Yanovych and V. Uruba, “Visualization of secondary flow in a corner of a channel”, AIP Conference Proceedings **2189**, 020003 (2019).
4. P. Saarenrinne and M. Piirto, “Turbulent Kinetic Energy Dissipation Rate Estimation from PIV Velocity Vector Fields”, Experiments in Fluids **29**, 300-307 (2000).
5. J. Sheng, H. Meng and R. O. Fox, “A Large Eddy PIV Method for Turbulence Dissipation Rate Estimation”, Chemical Engineering Science **55**, 4423-4434 (2000).
6. J. D. Jong et al, “Dissipation Rate Estimation from PIV in Zero-Mean Isotropic Turbulence” Experiments in Fluids **46**, 499-515 (2009).
7. D. Aronson and L. Löfdahl, “The Plane Wake of a Cylinder: Measurements and Inferences on Turbulence Modeling”, Physics of Fluids A **5**, 1433-1437 (1993).
8. Z. Hao, et al, “Approximations to Energy and Temperature Dissipation Rates in the Far Field of a Cylinder Wake”, Experimental Thermal and Fluid Science **32**, 791-799 (2008).
9. J. Mi, and R. Antonia, “Approach to Local Axisymmetry in a Turbulent Cylinder Wake” Experiments in Fluids **48**, 933-947 (2010).
10. V. Yanovych, D. Duda, V. Horáček and V. Uruba, “Research of a wind tunnel parameters by means of cross-section analysis of air flow profiles”, AIP Conference Proceedings **2189**, 020024 (2019).
11. V. Yanovych, D. Duda, V. Horáček and V. Uruba, “Creation of recombination corrective algorithm for research of a wind tunnel parameters”, AIP Conference Proceedings **2118**, 030050 (2019).
12. A. N. Kolmogorov, “The Local Structure of Turbulence in Incompressible Viscous Fluid for Very Large Reynolds' Numbers”, Doklady Akademiia Nauk SSSR **30**, 299: 301-305 (1941).